Strengthening of Recycled Aggregate Concrete Slender Column with CFRP

Ali F. A.[1, a *], Hasan Q. A.[1, b], and Mohammed D. H.[1, c]

[1]Civil Engineering Department, University of Technology, Baghdad, Iraq

[a]bce.21.04@grad.uotechnology.edu.iq, [b]40038@uotechnology.edu.iq, and [c]40041@uotechnology.edu.iq

*Corresponding author

Abstract. This piece provides an overview of an experimental program that tests the structural performance of slender recycled aggregate RAC columns that are externally restrained by carbon fiber reinforced polymer (CFRP composite system). To demonstrate that the CFRP strengthening system is one of the recommended effective techniques for making up for the reduction in load-carrying capacity caused by the use of 100% RCA in combination with the slenderness of column specimens, eight slender circular RC columns were modeled and tested. To more accurately predict the structural features of the RC thin column (the ultimate carrying weight, first cracking load, load-displacement curve, and load-strain response), the findings from experiments have been analyzed and monitored. The findings indicated that the type of transverse reinforcement and the amount of external strengthening impact the degree of improvement in column performance. The strength for the tied RC columns with 100% RCA confined by (25, 50, and 100) % CFRP increased by 5.5, 44.97, and 112.85%, respectively, compared to control columns with no CFRP confinement. Similar strength improvements are seen in spirally RC columns with 100% RCA and the same external confinement coverage ratio: 10.32, 42.81, and 113.51%.

Keywords: Slender Columns; Spiral Reinforcement; ties reinforcement; CFRP confinement.

1. INTRODUCTION

In an effort to address the challenges of climate change and environmental degradation, recycling concrete demolition waste is a process that is becoming more popular in civil engineering and construction [1]. As a result, governments and scholars are increasingly concerned with the essential issue of effectively utilizing building waste [2]. One method for recycling used concrete is recycled aggregate concrete (RAC). Waste concrete blocks were crushed to create recycled concrete aggregates (RCA), which partially or entirely replace natural aggregates (NA) in construction projects [3]. Despite this, regardless of these factors, some civil engineers and other related organizations continue to show caution to support the use of waste concrete as aggregate in recycled concrete. One explanation is that concrete constructed using recycled aggregate (RAC) performs worse than concrete prepared with natural aggregate (NAC) because it is frequently of lower quality [4,5].

Researchers [6–9] suggested using CFRP jackets to create FRP-confined RAC (FCRAC) composite members, which have been shown to improve the mechanical properties (strength and deformation capacity) of RAC due to the confining effect of FRP to address issues with RAC's shortcomings, such as shrinkage, enlarged creep of concrete due to large water absorption of RCAs, further to the reduced strength, modulus, and modulus of elasticity [10-12]. Several strengthening techniques have been suggested to improve the behavior of RAC, including physical and chemical treatment, [13,14] external confinement of steel tubes, [15, 16] or embedding profile steel [17]. Because of their high strength, high stiffness-to-weight ratio, and exceptional fatigue and corrosion resistance, FRP composite systems are being used in civil engineering more and more frequently [18-20].

On the other hand, column slenderness significantly affects the confinement action of slender columns, which must be considered in the design. Due to shifting functions and rising loads, these columns need to be strengthened. The study on CFRP-confined circular RC columns with greater slenderness is still quite limited, in contrast to the many experiments that have already been conducted on axially loaded short RC columns. The slenderness ratio is one of the crucial variables affecting the axial behavior of thin circular RC columns confined in CFRP and regulating the lateral constraint effect produced by CFRP tubes. [21]. It is simple to apply the CFRP sheet to reinforced concrete columns. The CFRP sheet offers cost efficiency and quick fabrication and is simple to apply to reinforced concrete columns. Abdallah et al. [22] investigated how thin CFFT columns behaved concerning axial stability. The findings demonstrated that when the slenderness ratio rises from 8 to 20, the specimens' carrying capacities drop by 22%. The eccentric compressive behavior of 10 circular RC columns with a diameter of 300 mm and H/D ratios ranging from 3 to 11 was researched by Xing et al. [23], and the results showed that the final bearing capacity of specimens decreased quickly as the eccentricity or slenderness ratio increased. Furthermore, numerous experimental studies on RC columns enclosed in CFRP have shown that doing so can improve the slender columns' ductility and strength [24]. Additionally, it has been noted in these studies that increasing the load eccentricity and/or column slenderness typically results in a decrease in the column's load capacity [25-27].

2. RESEARCH METHODOLOGY

Eight specimens were tested with a 100% RCA replacement percentage in order to examine the effect of CFRP strips and jackets as a compensating component to develop the strength and ductility of RC slender columns made with RCA. Four CFRP confinement percentages (0, 25, 50, and 100%) identified from A to D were used for this purpose. As a result, every couple of columns in the chosen percentage are tied and spirally reinforced.

The steps that make up this investigation's research approach are as follows:

- The RCA was obtained by handling waste concrete specimens with an electric hammer crusher machine and then by several sieves to get a precise grade similar to the used NCA.
- Plenty of concrete mixes were designed to achieve the target compressive strength.
- Casting process and curing of test columns for 28 days by immersing them in clan tap water basins.
- Strengthening columns with CFRP confinement system (strips, sheets, and resin).
- A testing program was made to determine the specimens' physical, mechanical, and structural parameters. The slump test was made for the concrete mixes in the fresh state to ensure the precise consistency of the mix. Standard tests such as compressive and tensile strength, elastic modulus, and the rapture modulus were determined for the control specimens in the hardened phase and after the curing of the concrete. Axial capacity, failure mode, and first crack investigation were achieved for the concrete column specimens.

3. MATERIALS

The recycled coarse aggregate is prepared by collecting waste concrete samples from laboratory test cubes and cylinders that exhibit a compressive strength of approximately 25-35 MPa, then breaking them with a mechanical hammer and crushing them to the required size using the crusher machine. The next process was grading the RCA with maximum particles of about 10 mm. Table 1 illustrates the physical properties of the used aggregate (RCA and natural sand NS).

Table 1: The physical properties of aggregate.

Aggregate Type	Specific Gravity	SO_3 Sulfate Content %	Absorption %	Fineness modulus
RA	2.42	0.06	3.67	6.65
NS	2.55	0.08	2.78	2.58

Throughout this study, all specimens, including cylinders, prisms, and RC slender column specimens, were cast using ordinary Portland cement (OPC), which is acceptable and identical to Iraqi specification No. 5/1984 [11]. Steel bars (deformed type) with an 8 mm diameter were utilized for longitudinal reinforcement, and bars with a 4 mm diameter were employed for transverse reinforcement. American Standard Specification A615/A615M [12] states. To retain the capacity of the available testing equipment at 28 days, the desired compressive strength of the concrete mix was set at roughly 25 MPa for normal strength concrete NSC. The current experiment employed various trial mixes to find the ideal mixture. The mix proportions for the concrete mix used in this experiment are shown in Table 2.

Table 2: The mix proportions (kg/m^3).

% of RCA	Cement (kg)	Sand (kg)	Gravel		Water (kg)	W/C
			NCA	RCA		
100	440	575	0	1096	200	0.45

A unidirectional woven fabric of CFRP components (strips and sheets) with mid-range tensile strengths was used to strengthen RC columns and develop their ductility. Teknowrap–300 contains 99% black carbon fibers of total area weight with 1% white thermoplastic heat-set fibers to maintain fiber stability. This experiment used two components of the bonding material (Teknobond–300 Tix Epoxy Adhesive) to perform the CFRP wrapping process. The white resin (part A) was mixed four times with the gray Hardener (Part B) at a mixing ratio of (3.85/1.15) by weight, then kept for seven days in normal air conditions to gain appropriate strength (due to manufacturer). Figure 1 shows the used CFRP wrap and resin, while Tables 3 and 4 clarify the product properties and the epoxy properties listed by the provider datasheet.

Table 3: CFRP properties characteristics.

Area Weight (g/m^2)	300 ± 10 (carbon fiber only)
Dry Fiber Density (g/m^3)	1.76 (based on fiber content)
Laminate Nominal Thickness (mm)	0.17 (based on total carbon content)
Laminate Nominal Cross Sectional Area (mm^2)	170 (per m width)
Modulus of Elasticity in Tension (MPa)	≥ 230,000 MPa
Fiber Tensile Strength (MPa)	≥ 4,900 MPa
Elongation at break (%)	2.1

Table 4: Epoxy adhesive product characteristics.

Mixture Ratio (by Weight)	3,85 units A: 1,15 units B
Consumption	1-1,15 kg/m for 300 g/m2
Applicable Ground Temperature	(+5°C) - (+35°C)
The density of mixed epoxy (Kg/L)	1.27 ± 0.03 kg/l
Tensile Strength (MPa)	≥ 30.0 (27 days at +20°C and 50% R.H)
Compressive Strength (MPa)	≥ 80.0 (27 days at +20°C and 50% R.H)
Flexural Strength (MPa)	≥ 40.0 (27 days at +20°C and 50% R.H)
Concrete Adhesion (N/mm^2)	≥ 4.0 (Rapture from concrete)

Figure 1: Teknowrap-300® product and Teknobond=300 Tix® Product.

4. COLUMN SPECIMENS

Throughout this study, 14 slender RC columns were modeled and tested. The columns were cast with a 1200 mm total unsupported length and a 150 mm diameter circular cross-section. With a slenderness ratio klu/r of 32, slender columns were created to take the slenderness effect into account. The dimensions are thought to fall within the laboratory testing machine's carrying loading range. For the purpose of preventing the direct impact of the axial loads on the primary reinforcing steel bars, each RC thin specimen had a concrete cover that extended 15 mm from all column surfaces. Up until the failure, axial compression load was the applied loading. According to how the transverse reinforcement was achieved (ties or spiral sets), Figure 2 illustrates structural details. Column specimens were identified with a series of letters and numbers. The first two letters (NA or RA) refer to the type of coarse aggregate (natural or recycled), and the following letter (T or S) indicates the type of transverse reinforcement of the column (tied or spirally reinforced). The numbers (25, 50, or 100) represent the percentage of aggregate replacement, and the last letter (A) means that there is no CFRP confinement. Figure 3 shows the CFRP strengthening schemes.

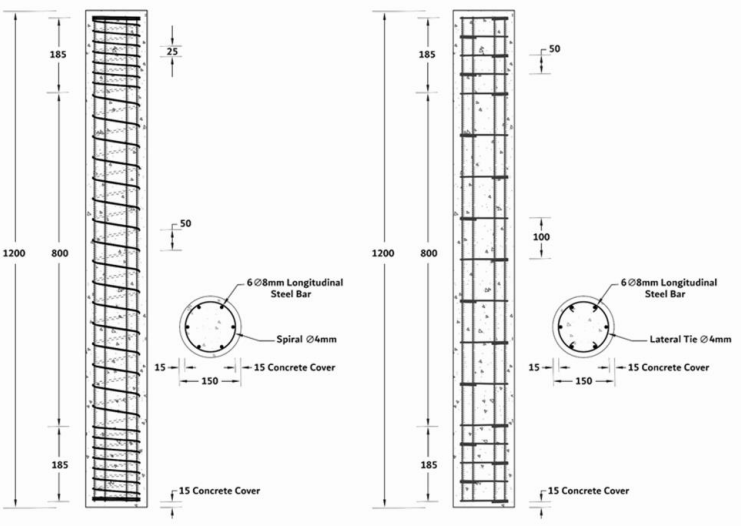

Figure 2: Structural details of slender columns with tied and spiral transverse reinforcement.

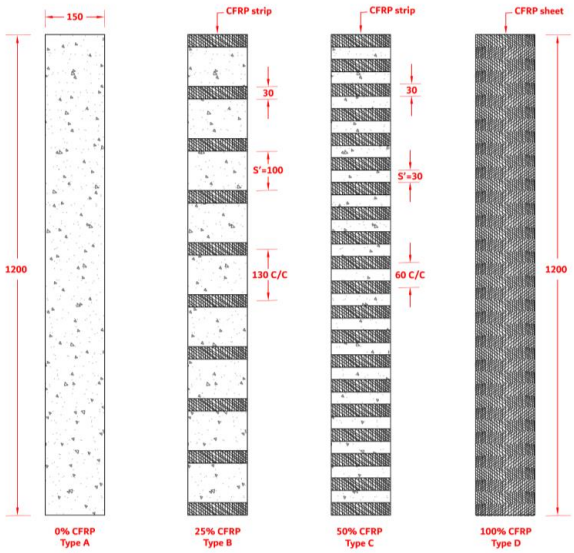

Figure 3: Types of CFRP strengthening schemes (units: mm).

5. TESTING PROGRAM

The RC column specimens were subjected to failure under a compression axial loading test with an AVERY machine with a compression capacity of about 2500 kN. The test was performed in the Construction Laboratory of the Civil Engineering Department at the University of Technology. Each column specimen was located carefully in the testing machine to ensure that the column specimen's axis coincides with the testing machine's axis. The axial loading results were recorded using a Load Cell of about 100 kN capacity. A linear voltage displacement transducer (LVDT) measured the longitudinal and lateral displacement. The longitudinal and lateral strains were recorded using two linear strain gauges located at the middle height of the columns. All LVDTs, strain gauges, and the load cell were connected to a data logger machine to save the test readings. Two steel collars (steel rings) with a height of 50 mm and thickness of 10 mm were placed at the top and bottom ends of the column before the loading process to avoid premature failure and enforce the stresses to be concentrated far away from the ends. The average increment of the load was gradually at a continual rate of 10 kN/sec until failure. The testing results and data were all recorded using the LabVIEW system with a rate of 80 readings per second. Figure 4 shows the procedure for testing RC column specimens.

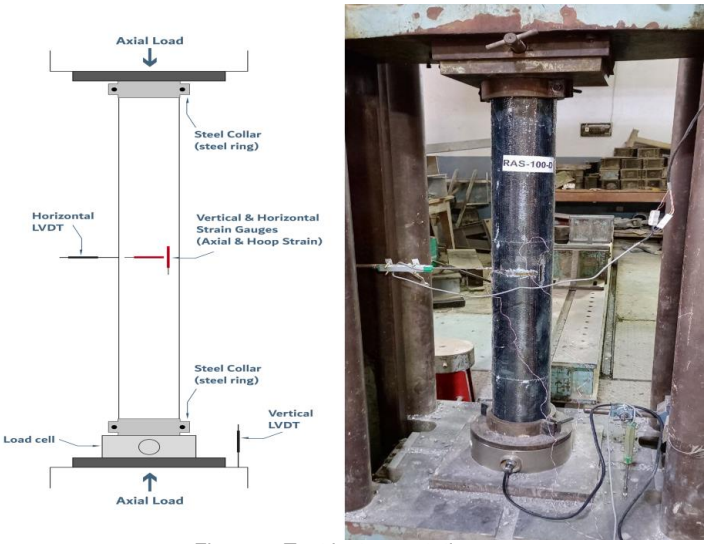

Figure 4: Test instrumentations.

6. RESULTS AND DISCUSSION

All RC column specimens in this investigation were tested under concentric axial loading until failure. The first cracking load of each column specimen during the testing was registered to document the moment of appearance of the first crack and to record the value of the applied load at this moment. Table 5 illustrates the first cracking load (P_{cr}) and the ultimate load (P_u) for the tested tied and spirally reinforced columns.

Table 5: First cracking and ultimate loads results.

Col-ID	Ultimate Capacity, P_{ult} (kN)	First Cracking Load, P_{cr} (kN)	P_{cr}/P_{ult} (%)
RAT100-A	476.03	385.95	0.81
RAS100-A	511.34	418.49	0.82
RAT100-B	502.22	428.45	0.85
RAS100-B	564.10	468.31	0.83
RAT100-C	690.08	573.04	0.83
RAS100-C	730.23	627.73	0.86
RAT100-D	1013.22	-*	-
RAS100-D	1091.77	-*	-

* No visible cracks can be observed in columns fully wrapped with CFRP sheets.

6.1 CFRP Confinement Effect on the First Cracking Load and the Ultimate Carrying Load

Three main external confinement ratios (25, 50, and 100%) were used in this investigation. Table 6 shows comparison values for the effect of strengthening with CFRP wrapping on the first cracking load and the ultimate carrying load. It was noticed that there was a slight increase in the ultimate capacity and the first cracking load for the tested column specimens. For column specimens strengthened with 25% of CFRP wrapping, it was noted that increases in the ultimate carrying load and the first cracking load were 11.01 and 11.9%, respectively, for tied and spirally RC specimen (RAS100-B) and (RAT100-B), in comparison to the 100% RCA control column specimens with no CFRP wrapping (RAT100-A and RAS100-A). The results of 50% strengthened column specimens with CFRP show higher values for the ultimate carrying load and the first cracking load. The results were 48.48 and 50% for tied and spirally RC specimens (RAT100-C) and (RAS100-C).

Conversely, the ultimate capacity increase was much higher for column specimens fully wrapped with CFRP sheets (RAT100-D and RAS100-D). The ultimate carrying load values increase was 112.85 and 113.51%, respectively. No visible first cracking load was recorded for all column specimens with 100% CFRP confinement.

Table 6: First cracking and ultimate loads results.

Col-ID	% of CFRP	P_{ult} (kN)	% P_{ult} Increase	P_{cr} (kN)	% P_{cr} Increase
RAT100-A	0	476.03	-	385.95	-
RAT100-B	25	502.22	5.50%	428.45	11.01%
RAT100-C	50	690.08	44.97%	573.04	48.48%
RAT100-D	100	1013.22	112.85%	-*	-
RAS100-A	0	511.34	-	418.49	-
RAS100-B	25	564.1	10.32%	468.31	11.90%
RAS100-C	50	730.23	42.81%	627.73	50.00%
RAS100-D	100	1091.77	113.51%	-*	-

* No visible cracks can be observed in columns fully wrapped with CFRP sheets.

6.2 Behavior and Failure Pattern

Cracks began to appear in non-strengthened slender RC columns with 100% RCA replacement content (RAT100-A) and (RAS100-A), respectively, at 81 and 82% of their maximum carrying capacities. More fractures expanded and collapsed by explosion pattern around the tops of the tested region with each increase in applied loading, with the exception of RAS100-A, which ruptured in the middle of the height due to longitudinal steel reinforcement buckling in addition to ties and spirals breaking. For slender column specimens enhanced with 25% CFRP sheets (strengthening scheme type B), the cracks began in the area left exposed by CFRP strips at about 85 and 83% of their ultimate capacities for tied and spirally RC columns (RAT100-B) and (RAS100-B), respectively. As the load increases, more cracks appear and become more obvious. In addition to this, column specimens with CFRP layers that ruptured towards the top also caused concrete to crush.

For tied and spirally RC columns (RAT100-C and (RAS100-C), the first cracks appeared at about 83 and 86% of their ultimate capacity, respectively, when the vertical spacing between CFRP layers was reduced from 130 to 60 mm c/c, or 50% of CFRP sheets. As the applied load increased, more cracks appeared and became more pronounced. Finally, the rupturing of the CFRP layers in the column sample causes more concrete to be crushed close to the column's middle. Due to the CFRP sheets' coverage of the concrete area in the fully

wrapped slender column specimens (100 percent CFRP, strengthening scheme type D), no cracks appeared. Particularly when the applied loading surpasses about 50% of the ultimate capacity, the strong bonding between the CFRP layer and the concrete surface of specimens (RAT100-D) and (RAS100-D) causes audible cracks due to the production of micro-cracks and the breakdown of resin bonds. At the final stage, there was a very loud explosion sound. The column specimens behaved differently than the previously tested columns. They failed by lateral deflection with concrete crushing in all directions, buckling of 72 longitudinal steel reinforcements, and breaking transverse reinforcing ties and spirals. The full strengthening scheme affects the slenderness of column specimens by acting as a restraint system to the extended constrained concrete beyond the thin column's outer limit and relieving the restraint pressure when the CFRP jackets reach their rupture point, which results in concrete crushing. For column specimens with all CFRP percentages, there was good bonding between the CFRP sheet and the concrete outside surface, and no notable fiber de-bonding was visible up to the ultimate load. Figure 5 displays the failure patterns of columns with tied reinforcement.

Figure 5: Failure patterns of columns with tied reinforcement.

6.3 Load-Displacement and Load-Strain Relationship

The performance of slender CFRP-confined circular RC columns was assessed using the load vs. deflection curves with constant RCA percentage and slenderness ratio, as illustrated in Figure 6. The load-deflection curve has essentially two steps. The first stage curvature of the columns in the elastic ascending stage had a better shape due to the utilization of CFRP strips and jackets. As the CFRP confinement percentage rises, the columns become more stable. Even though the correlation between the applied loading and the longitudinal and lateral displacement showed the same ascending pattern, it is obvious that the CFRP confinement ratio increases the flexural stiffness of column specimens, especially for fully wrapped column specimens. Spiral transverse reinforcement allows RC columns to withstand more applied loading with respect to longitudinal displacement than tied reinforced columns, leading to higher flexural stiffness values on the load-displacement curve. This is similar to how the type of transverse reinforcement affects RC column stiffness.

The tendency for deformation of slender RC columns strengthened with CFRP strips and coats increased depending on the CFRP confinement ratio. The measured strain reduces with increasing CFRP confinement % as the applied axial loading rises in the elastic stage, and this pattern retains up until the ultimate stage is reached. Similarly, the type of transverse reinforcement affected the ability of RC columns to deform; RC columns with spiral reinforcement have a higher deformation capacity. The effects of CFRP confinement on the load-strain behavior of slender RC columns are shown in Figure 7.

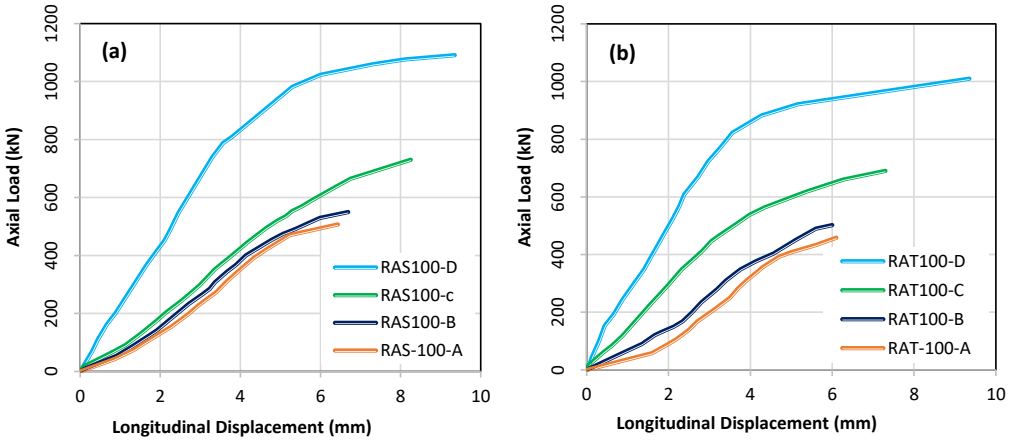

Figure 6: Load-Longitudinal displacement curves for a: tied, and b: spirally RC slender columns.

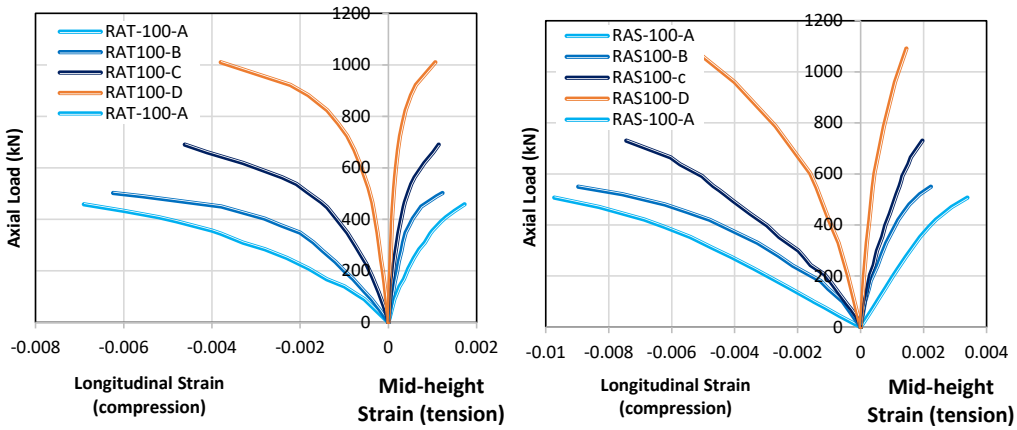

(a) (b)

Figure 7: Load-strain curves for a: tied and b: spirally RC slender columns.

For the calculations of the load carrying capacity for fully or partially CFRP-strengthened columns loaded by concentric axial load (regardless of the reduction factors for ties 0.8ø and 0.85ø for spirals), the American Code Institute's proposed equation (1) may be used (ACI Committee 440.2R-17) [30]:

$$Po = 0.85\,\mathrm{f'cc}\,(Ag - Ast) + \mathrm{fy}\,Ast \quad (1)$$

Using eq. (2) and the implications of an extra reduction factor ψf = 0.95, it is possible to predict the ultimate strength of concrete that is externally constrained by CFRP $f'cc$ where it can be calculated by:

$$f'cc = f'c + \Psi f\ 3.3\ ka\ \mathrm{fl} \quad (2)$$

Where $f'c$ is the compressive strength of cylindrical unconfined concrete, Ka is the "shape factor" (the highest possible value of Ka is 1.00 for circular cross-sectional columns), fl is the maximum external lateral confining pressure provided by the CFRP jacket, and it can be calculated using equation (3).

$$\mathrm{fl} = 0.5\,\rho j\ \mathrm{ke}\ \mathrm{fCFRP} \quad (3)$$

$$\rho j = \frac{4t}{D} \quad (4)$$

f_{CFRP} is the ultimate tensile strength of the carbon fiber fabric, t is the nominal thickness of the CFRP jacket, and D is the cross-sectional dimension of the confined column. ρj indicates the volumetric ratio of the external CFRP confinement. To calculate the effective lateral confining pressure of partial wrapping, a confinement efficiency factor (ke) was employed:

$$\mathrm{ke} = \frac{\left[1-\frac{s'}{2\mathrm{D}}\right]^2}{1-\rho s g} \approx \left[1-\frac{s'}{2\mathrm{D}}\right]^2 \quad (5)$$

Where s' is the main reinforcing steel bars ratio in relation to the gross cross-sectional area and s′ is the clear spacing between the CFRP wraps. Table 7 compares experimental testing findings for the maximum carrying load to the estimated load capacity determined in accordance with ACI Committee 440.

Table 7: First cracking and ultimate loads results.

Col-ID	Cylindrical Concrete Compressive Strength		Ultimate Load Carrying Capacity		Factor of Safety (P_{exp} / P_{cal})
	Unconfined f'_c (MPa)	Confined f'_{cc} (MPa)	Calculated P_{cal} (kN)	Experimental P_{exp} (kN)	
RAT100-A	24.45	-	560.72	476.03	0.85
RAS100-A	24.45	-	560.72	511.34	0.91
RAT100-B	24.45	45.77	700.53	502.22	0.72
RAS100-B	24.45	45.77	700.53	564.10	0.81
RAT100-C	24.45	41.72	815.53	690.08	0.85
RAS100-C	24.45	41.72	815.53	730.23	0.90
RAT100-D	24.45	33.92	875.31	1013.22	1.16
RAS100-D	24.45	33.92	875.31	1091.77	1.25

Table 7 shows that when the CFRP confinement ratio is not 100%, the experimental results of the axial compressive strength were higher than the predicted values for columns (unsafe specimens, P_{exp} / P_{cal} < 1). In contrast, this reduction in the factor of safety of column specimens due to the full replacement of NCA by RCA further to the slenderness effect was improved by using 100% CFRP confinement. In contrast to conventional linked RC columns, spirally RC columns showed a higher Load load-carrying capacity than expected computed results (higher safety factor). This is applicable for all CFRP confinement percentages.

7. CONCLUSIONS

Based on the experimental results collected throughout this investigation, there are several conclusions were gathered as the following:

- Strengthening RC columns with CFRP wrapping percentages (25, 50, and 100%) increased the ultimate capacity, especially for fully wrapped columns which provided an excellent confining system and developed the first crack propagation.
- Using 100% CFRP jackets improved the safety reduction factor, resulting in the full replacement of NCA with 100% RCA content, further to the slenderness effect. The expected results were 16% and 25% higher than predicted for tied and spirally RC columns.
- The performance of CFRP-wrapped columns is better when spiral transverse reinforcement is used compared to ties reinforcement for all CFRP confinement percentages (at fixed RCA content).
- The load-displacement curve of RC slender columns shows higher flexural stiffness values with increased CFRP wrapping percentage and spiral reinforcement, further improving the curve's shape at all loading stages.
- The load-strain response of RC slender columns improved by the increase of CFRP confinement percentage, which reduced the deformations capacity, especially when 100% of CFRP ratios were used. Also, the use of spiral reinforcement decreases both lateral and longitudinal strains at the mid-height of the column.

REFERENCES

[1] Jiang T, Teng JG. Analysis-oriented stress–strain models for FRP–confined concrete. Eng Struct. 2007 Nov;29(11):68-86.
[2] Xu CY, Liu YJ, Zhang YM, Han LH, Su Y, Wu D. Seismic performance of RC beam-column edge joints reinforced with austenite stainless steel. Eng Struct. 2021 Jun;232(1):111824.
[3] Bakouregui AS, Shi Q, Wang J, Wu C, Yao W. Explainable extreme gradient boosting tree-based prediction of load-carrying capacity of FRP-RC columns. Eng Struct. 2021 Dec;245(1):112836.
[4] Nguyen H, Doan TM, Nguyen QD, Nguyen D. Efficient machine learning models for prediction of concrete strengths. Constr Build Mater. 2021 Dec;266(1):120950.
[5] Heitz T, Kanyilmaz A, Dorka U. Identification of an equivalent viscous damping function depending on engineering demand parameters. Eng Struct. 2019 Sep;188(1):637-649.
[6] Xiong MX, Li ZH, Li J, Li WF, Liu YB. FRP-confined steel-reinforced recycled aggregate concrete columns: Concept and behaviour under axial compression. Compos Struct. 2020 Dec;246(1):112408.

[7] Chen GM, Li Q, Guo HY, Li HJ, Li N. Compressive behavior of FRP-confined steel-reinforced high strength concrete columns. Eng Struct. 2020 Mar;220(1):110990.
[8] Huang L, Li X, Xiao Y, Li L, Wu Y, Liu W. Compressive behaviour of large rupture strain FRP-confined concrete-encased steel columns. Constr Build Mater. 2018 Oct;183(1):513-522.
[9] Ren FM, Cao SY, Zhou ZQ, Li LJ, Qian XQ, Li JH. Behaviour of FRP tube-concrete-encased steel composite columns. Compos Struct. 2020 Aug;241(1):112139.
[10] Feng P, Li Y, Zhang Y, Liu H, Zhou L, Huo Y. Mechanical behavior of concrete-filled square steel tube with FRP-confined concrete core subjected to axial compression. Compos Struct. 2015 Sep;123(1):312-324.
[11] Idris Y, Teng JG, Paramasivam P, Wong TC, Zhang JL. Behavior of square fiber reinforced polymer–high-strength concrete–steel double-skin tubular columns under combined axial compression and reversed-cyclic lateral loading. Eng Struct. 2016 Sep;118(1):307-319.
[12] Zhang B, Teng JG, Wang JY, Yao JJ, Chen JF. Experimental behavior of hybrid FRP–concrete–steel double-skin tubular columns under combined axial compression and cyclic lateral loading. Eng Struct. 2015 Dec;99:214-231.
[13] Hu Z, Zhou M, Yuan J, Lin T, Wang H. Experimental Study on Slender CFRP-Confined Circular RC Columns under Axial Compression. Appl. Sci. 2021 Nov;11(9):3968.
[14] Dundar C, Sen F, Dikmen N, Binici B. Studies on carbon fiber polymer confined slender plain and steel fiber reinforced concrete columns. Eng Struct. 2015 Dec;102(1):31-39.
[15] Abdallah MH, Al-Salloum YA, Alsayed SH, Almusallam TH. Experimental assessment and theoretical evaluation of axial behavior of short and slender CFFT columns reinforced with steel and CFRP bars. Constr. Build. Mater. 2018;181(1):535–550.
[16] Xing L, Cai J, Zhang Y, Chen X. Behavior of FRP-Confined Circular RC Columns under Eccentric Compression. J. Compos. Constr. 2020;24:04020030.
[17] Khan AR, Fareed S. Behaviour of recycled aggregates RC columns strengthened with CFRP under uniaxial compressive loadings. IOP Conf. Ser. Mater. Sci. Eng. 2019;596(1):012027.
[18] Khan AR, Memon RA, Fareed S, Kim H. Behaviour and Strength Prediction of Reinforced Recycled Aggregate Concrete Columns Confined with CFRP Wraps. Iran. J. Sci. Technol. Trans. Civ. Eng. 2021.
[19] Fareed S, Khan AR, Memon RA. Behaviour of Recycled Aggregate RC Columns Wrapped with CFRP Under Axial Compression. In: Procedia Structural Integrity. 10th International Conference on FRP Composites in Civil Engineering. 2022.
[20] Nguyen-Sy T, Wong HS, Anwar MP, Loo YC, Lee SL. Predicting the compressive strength of concrete from its compositions and age using the extreme gradient boosting method. Constr. Build. Mater. 2020;260(1):119757.
[21] Xu J, Wong HS, Anwar MP, Loo YC, Lee SL. Performance evaluation of recycled aggregate concrete-filled steel tubes under different loading conditions: Database analysis and modelling. J. Build. Eng. 2020;30(1):101308.
[22] Xu J, Wong HS, Anwar MP, Loo YC, Lee SL. Parametric sensitivity analysis and modelling of mechanical properties of normal- and high-strength recycled aggregate concrete using grey theory, multiple nonlinear regression and artificial neural networks. Constr. Build. Mater. 2019;211(1):479-491.
[23] Xu J, Wong HS, Anwar MP, Loo YC, Lee SL. Prediction of triaxial behavior of recycled aggregate concrete using multivariable regression and artificial neural network techniques. Constr. Build. Mater. 2019;226(1):534-554.
[24] Naderpour H, Kheyroddin A, Gandomi AH. Compressive strength prediction of environmentally friendly concrete using artificial neural networks. J. Build. Eng. 2018;16(1):213-219.
[25] Gholampour A, Gholampour F, Khaloo AR. New formulations for mechanical properties of recycled aggregate concrete using gene expression programming. Constr. Build. Mater. 2017;130(1):122-145.
[26] Behnood A, Ziari H, Asadi M, et al. Predicting modulus elasticity of recycled aggregate concrete using M5′ model tree algorithm. Construction and Building Materials. 2015;94(1):137-147.
[27] Duan ZH, Kou SC, Poon CS. Prediction of compressive strength of recycled aggregate concrete using artificial neural networks. Construction and Building Materials. 2013;40(1):1200-1206.
[28] Central Organization for Standardization and Quality Control. Iraqi Standard Specification for the Portland Cement, IQS (5). (translated from Arabic). 1984.
[29] ASTM International. ASTM A615/A615M – 15. Standard Specification for Deformed and Plain Carbon-Steel Bars for Concrete Reinforcement. 2015.
[30] ACI Committee 440.2R-17. Guide for the Design and Construction of Externally Bonded FRP Systems for Strengthening Concrete Structures. American Concrete Institute. 2017.